



HAL
open science

Daughter centrioles assemble preferentially towards the nuclear envelope in *Drosophila* syncytial embryos

Neil H J Cunningham, Imène B Bouhleb, Paul Conduit

► **To cite this version:**

Neil H J Cunningham, Imène B Bouhleb, Paul Conduit. Daughter centrioles assemble preferentially towards the nuclear envelope in *Drosophila* syncytial embryos. *Open Biology*, 2022, 10.1098/rsob.210343 . hal-03454293v2

HAL Id: hal-03454293

<https://hal.science/hal-03454293v2>

Submitted on 21 Jan 2022

HAL is a multi-disciplinary open access archive for the deposit and dissemination of scientific research documents, whether they are published or not. The documents may come from teaching and research institutions in France or abroad, or from public or private research centers.

L'archive ouverte pluridisciplinaire **HAL**, est destinée au dépôt et à la diffusion de documents scientifiques de niveau recherche, publiés ou non, émanant des établissements d'enseignement et de recherche français ou étrangers, des laboratoires publics ou privés.

2 **Daughter centrioles assemble preferentially towards the nuclear**
3 **envelope in *Drosophila* syncytial embryos**

4
5
6
7 Neil H. J. Cunningham^{1,§}, Imène B. Bouhlel^{1,§}, and Paul T. Conduit^{1,2,3}

8
9 ¹Department of Zoology, University of Cambridge, Downing Street, Cambridge, CB2
10 3EJ

11
12 ²Université de Paris, CNRS, Institut Jacques Monod, F-75013, Paris, France.

13
14 § These authors contributed equally to this work.

15
16 ³Corresponding author

17 Paul T. Conduit

18 Institut Jacques Monod

19 CNRS - Université de Paris

20 15 rue Hélène Brion

21 75013 Paris

22 France

23 0033 (1) 57 27 80 95

24 paul.conduit@ijm.fr

25 ORCID: 0000-0002-7822-1191

26
27 Keywords: Centrosome, centriole, centriole duplication, *Drosophila*, microtubules.

28 **Abstract**

29 Centrosomes are important organisers of microtubules within animal cells. They
30 comprise a pair of centrioles surrounded by the pericentriolar material (PCM), which
31 nucleates and organises the microtubules. To maintain centrosome numbers,
32 centrioles must duplicate once and only once per cell cycle. During S-phase, a single
33 new “daughter” centriole is built orthogonally on one side of each radially symmetric
34 “mother” centriole. Mis-regulation of duplication can result in the simultaneous
35 formation of multiple daughter centrioles around a single mother centriole, leading to
36 centrosome amplification, a hallmark of cancer. It remains unclear how a single
37 duplication site is established. It also remains unknown whether this site is pre-defined
38 or randomly positioned around the mother centriole. Here, we show that within
39 *Drosophila* syncytial embryos daughter centrioles preferentially assemble on the side
40 of the mother facing the nuclear envelope, to which the centrosomes are closely
41 attached. This positional preference is established early during duplication and
42 remains stable throughout daughter centriole assembly, but is lost in centrosomes
43 forced to lose their connection to the nuclear envelope. This shows that non-
44 centrosomal cues influence centriole duplication and raises the possibility that these
45 external cues could help establish a single duplication site.

46

47

48

49

50

51

52 **Introduction**

53 Centrosomes are important microtubule organising centres (MTOCs) within animal
54 cells, best known for organising the mitotic spindle poles during cell division (Conduit
55 et al., 2015b). They typically comprise an older “mother” and younger “daughter” pair
56 of barrel-shaped microtubule-based centrioles. While centriole structure varies
57 between species and cell type (Loncarek and Bettencourt-Dias, 2018), they all display
58 a 9-fold radial symmetry, with an inner “cartwheel” structure supporting the assembly
59 of 9 microtubule triplets, doublets or singlets that make up the centriole wall. The
60 mother centriole recruits and organises a surrounding pericentriolar material (PCM),
61 which contains the necessary microtubule-associating and signalling proteins required
62 for centrosome function (Woodruff et al., 2014). The mother centriole also templates
63 the assembly of the daughter centriole in a process called centriole duplication
64 (Banterle and Gönczy, 2017; Firat-Karalar and Stearns, 2014; Fu et al., 2015). This
65 occurs after cell division, when each daughter inherits a single centrosome containing
66 a disengaged mother-daughter centriole pair. The daughter centriole is converted into
67 a mother and both mothers support the orthogonal assembly of a new daughter
68 centriole at their proximal end during S-phase. The two mother-daughter centriole
69 pairs break apart during G2/M-phase to form two centrosomes, which mature by
70 recruiting more PCM in preparation for mitosis. During mitosis, the two centrosomes
71 each organise one pole of the bipolar spindle and towards the end of mitosis the
72 centrioles disengage in preparation for a new round of duplication in the following cell
73 cycle.

74

75 In most cell types, centrioles duplicate once per cell cycle during S-phase and it is this
76 “once and only once” duplication event that maintains centrosome numbers through
77 multiple cell divisions (Nigg and Holland, 2018). Failure to duplicate the centrioles
78 during S-phase results in the inheritance of a centrosome with a single centriole, which
79 cannot then split to form two centrosomes. This leads to monopolar spindle formation
80 and cell cycle arrest. In contrast, multiple centrosomes form if mother centrioles
81 template the assembly of more than one daughter centriole and this leads to multipolar
82 spindle formation in the next cell cycle. Multipolar spindles can result in cell death or
83 they can be transformed into bipolar spindles that harbour erroneous kinetochores

84 attachments, leading to lagging chromosomes and chromosome instability (Basto et
85 al., 2008; Ganem et al., 2009; Godinho and Pellman, 2014; Nigg and Holland, 2018).
86 Centrosome amplification is strongly associated with cancer progression, with
87 chromosome instability and increased centrosome signalling being possible causal
88 links (Anderhub et al., 2012; Basto et al., 2008; Denu et al., 2016; Godinho et al., 2014;
89 Godinho and Pellman, 2014; Mittal et al., 2021; Salisbury et al., 2004).

90

91 Seminal studies in *C. elegans* identified a core set of proteins necessary for centriole
92 duplication: the kinase ZYG-1 and the large coiled-coil proteins SPD-2, SAS-4, SAS-
93 5 and SAS-6 (Delattre et al., 2006; Leidel and Gönczy, 2003; O'Connell et al., 2001;
94 Pelletier et al., 2006). Homologues in *Drosophila* (Sak/Plk4, Spd-2, Sas-4, Ana2 and
95 Sas-6) and human cells (PLK4, CEP192, CPAP, STIL and SAS-6) were subsequently
96 identified and, with the exception of *Drosophila* Spd-2 (Dix and Raff, 2007), shown to
97 also be essential for centriole duplication (Basto et al., 2006; Bettencourt-Dias et al.,
98 2005; Dammermann et al., 2004; Habedanck et al., 2005; Kim et al., 2013; Leidel et
99 al., 2005; Sonnen et al., 2013; Stevens et al., 2010; Tang et al., 2011; Terra et al.,
100 2005). The role of worm SPD-2, which is to recruit ZYG1/PLK4, is played instead by
101 *Drosophila* Asterless (Asl) (Blachon et al., 2008; Dzhindzhev et al., 2010), and the
102 human homologues of Asl (CEP152) is also required for centriole duplication (Blachon
103 et al., 2008; Cizmecioglu et al., 2010; Hatch et al., 2010), functioning together with the
104 human homologue of SPD-2 (CEP192) to recruit PLK-4 (Kim et al., 2013; Park et al.,
105 2014; Sonnen et al., 2013).

106

107 A large number of studies are producing a clear picture about how each of these
108 proteins contributes to centriole assembly (reviewed in (Arquint and Nigg, 2016; Firat-
109 Karalar and Stearns, 2014; Fu et al., 2015; Yamamoto and Kitagawa, 2021). In
110 essence, CEP192/SPD-2 and/or CEP152/Asl recruit the master kinase PLK-4 to the
111 wall of the mother centriole where it regulates the recruitment of STIL/Ana2 and SAS-
112 6 and then CPAP/Sas-4 to form the daughter centriole. A key feature is that daughter
113 centriole assembly occurs on only one side of the radially symmetric mother centriole,
114 and this relies on localising PLK4, SAS-6 and STIL/Ana2 to a single spot on the side
115 of the mother. The problem is that CEP192/SPD-2 and CEP152/Asl localise as a ring

116 around the mother centriole and thus PLK4 is also initially recruited in a ring-like
117 pattern (Kim et al., 2013; Park et al., 2014; Sonnen et al., 2013). In order for just a
118 single daughter centriole to form, this ring of PLK4 must therefore be converted to a
119 'dot', which marks the site of centriole duplication. Failure of PLK4 to undergo this
120 'ring-to-dot' conversion results in multiple daughter centrioles forming around the
121 mother centriole and this leads to centrosome amplification (Brownlee et al., 2011;
122 Habedanck et al., 2005; Klebba et al., 2013; Kleylein-Sohn et al., 2007; Ohta et al.,
123 2014). Ring-to-dot conversion of PLK4 is thought to be largely self-controlled, as it
124 involves the auto-phosphorylation of a degron within PLK4 (Cunha-Ferreira et al.,
125 2013, 2009; Guderian et al., 2010; Holland et al., 2010; Klebba et al., 2013; Rogers et
126 al., 2009; Sillibourne et al., 2010), and could also depend on the ability of PLK4 to self-
127 assemble, a property that is regulated by auto-phosphorylation and that protects PLK4
128 from degradation (Gouveia et al., 2018; Park et al., 2019; Yamamoto and Kitagawa,
129 2019). Nevertheless, ring-to-dot conversion is likely also influenced by the binding of
130 STIL/Ana-2, which increases PLK4 activity (Arquint et al., 2015; Moyer et al., 2015)
131 and protects PLK4 from degradation (Arquint et al., 2015; Ohta et al., 2014). In human
132 cells, PLK4 is observed as an asymmetric punctate ring prior to the recruitment of
133 STIL, suggesting that initial symmetry breaking is independent of STIL, although the
134 full ring-to-dot conversion occurs only once STIL and SAS-6 have been recruited (Kim
135 et al., 2013; Ohta et al., 2018, 2014; Park et al., 2014; Yamamoto and Kitagawa,
136 2019). In flies, Ana2 recruitment is the first observed symmetry breaking event
137 (Dzhindzhev et al., 2017). Mathematical models can explain how the properties of
138 PLK4, with or without the help of STIL/Ana2, can lead to the symmetry breaking ring-
139 to-dot transition (Leda et al., 2018; Takao et al., 2019).

140

141 While various studies have focussed on understanding how symmetry breaking is
142 achieved, it remains unknown whether the site of daughter centriole assembly is
143 randomly assigned or not. We decided to investigate this using *Drosophila* syncytial
144 embryos as a model system. These embryos go through rapid and near-synchronous
145 rounds of S-phase and then mitosis with no intervening gap phases. The nuclear
146 envelope does not fully break down during mitosis and the centrosomes remain closely
147 attached to the nuclear envelope throughout each cycle. At the end of mitosis / start

148 of S-phase, mother and daughter centrioles separate with the daughter converting to
149 a mother and both centrioles quickly migrate around the nuclear envelope to form two
150 new centrosomes that will organise the next round of mitosis. During S-phase, each
151 mother centriole templates the formation of a new daughter centriole, with only the
152 mother centriole organising PCM (Conduit et al., 2015a, 2010). Towards the end of
153 mitosis, the centrioles disengage and the daughter centrioles are converted to mothers
154 by the addition of Asl, allowing them to begin recruiting PCM and initiate centriole
155 duplication in the next cycle (Conduit et al., 2010; Novak et al., 2014).

156

157 Using a dual-colour FRAP approach along with super-resolution Airyscan imaging, we
158 show here that daughter centrioles preferentially assemble on the side of the mother
159 centriole facing the nuclear envelope. By tracking duplication events throughout S-
160 phase, we show that this preferential positioning of the daughter centriole with respect
161 to the nucleus occurs from the early stages of centriole formation and remains
162 relatively stable throughout the cycle. Using a point mutation in the key PCM protein
163 Centrosomin (Cnn), we show that this preferential positioning towards the nuclear
164 envelope is lost in centrosomes that have detached from the nuclear envelope.
165 Collectively, these observations suggest that the site of centriole duplication is
166 influenced by the nuclear envelope and raise the possibility that cues external to the
167 centriole duplication machinery may influence and help control centriole duplication.

168

169 **Results**

170

171 The site of daughter centriole assembly is non-random with respect to cell geometry

172 To address whether the site of daughter centriole formation is pre-defined or randomly
173 assigned during centriole duplication, we turned to the *Drosophila* syncytial embryo.
174 In these embryos hundreds of nuclei and centrosomes undergo rapid cycles of division
175 (~8-15 min per cycle) in near synchrony, alternating between S-phase and M-phase
176 without gap phases. At around division cycle 9 the nuclei and centrosomes migrate to
177 the cell cortex and their divisions can be readily imaged with a fluorescence-based
178 microscope until they pause in cycle 14. Mitotic spindles form parallel to the cortex
179 such that they align along the X-Y imaging plane. The mother centrioles also have a
180 regular alignment; their proximal-distal (end-to-end) axis is aligned orthogonally to the
181 spindle axis such that mother centrioles point along the Z imaging axis. Newly forming
182 daughter centrioles grow along the X-Y imaging axis. This regular alignment of the
183 centrioles in theory allows one to record the position of the daughter centriole relative
184 to other cellular structures, such as the mitotic spindle axis. *Drosophila* centrioles are
185 relatively small, however, meaning that duplicating mother-daughter centriole pairs
186 cannot be resolved using “standard” confocal microscopy. We therefore developed a
187 method to estimate the location of the centrioles within an engaged mother-daughter
188 centriole pair by performing dual-colour Fluorescence Recovery After Photobleaching
189 (FRAP) experiments. This relies on the fact that PCM proteins, such as Spd-2, Asl or
190 Cnn, are dynamically recruited around the mother, but not the daughter, centriole,
191 while the centriole protein Sas-4 is dynamically recruited to the growing daughter, but
192 not the mother, centriole (Conduit et al., 2015a). By tagging a PCM protein and Sas-4
193 with different coloured fluorophores and then photobleaching during S-phase, the
194 centroids of the recovering fluorescent signals can be used to estimate the relative
195 positions of the mother (PCM signal) and daughter centrioles (Sas-4 signal) (Figure
196 1A). We used this approach to compare the position of the growing daughter centriole
197 relative to the mother centriole and the future spindle axis (Figure 1B).

198

199 To begin with, we used Spd-2-GFP and Sas-4-mCherry as our mother and daughter
200 centriole markers, respectively. We photobleached either one centrosome from a

201 separating centrosome pair during early S-phase (when Sas-4 starts to be
202 incorporated at the newly forming daughter centriole) or we photobleached a single
203 centrosome in late M-phase, just prior to centrosome splitting, daughter centriole
204 assembly and Sas-4 recruitment, and monitored the two resulting centrosomes in the
205 following S-phase. Both cases result in centrosomes where Spd-2-GFP recovers only
206 around the mother centriole and Sas-4-mCherry recovers only at the growing daughter
207 centrioles during S-phase, but the latter case generates two centrosomes that can be
208 analysed. We recorded the centroids of the recovering fluorescent signals in mid to
209 late S-phase once the centrosomes had reached their final positions on the opposite
210 side of the nuclear envelope. Waiting until the centrosomes had fully separated
211 allowed us to use the future spindle axis (a line drawn between the paired
212 centrosomes) as a spatial reference point with which to compare the position of
213 daughter centriole assembly (Figure 1B). We analysed a total of 121 centrosomes
214 from 16 embryos and collated the results. Strikingly, the positions of daughter
215 centrioles were not evenly distributed relative to the future spindle axis (positive Y axis
216 in Figure 1C). A frequency distribution of the angles of the daughter centrioles relative
217 to the future spindle axis showed displayed a Normal distribution around the 0° angle
218 (Figure S1A,B) (passed all 4 normality tests in Prism) i.e. the daughter centrioles had
219 a preference to be close to the 0° angle and were not evenly distributed around the
220 mother centriole (Chi-square=44.52, df=11, p<0.0001), as would be expected if
221 daughter centriole positioning were random. The data can also be represented by a
222 Rose Plot, where each segment corresponds to a duplication event and its position
223 corresponds to the angle from the future spindle axis (Figure 1D). 95 of 121 (78.51%)
224 daughter centrioles were assembled within 90 degrees of the future spindle axis (blue
225 segments, Figure 1D), while only 26 (21.49%) were assembled more than 90 degrees
226 from the future spindle axis (red segments, Figure 1F) (Binomial Wilson/Brown test,
227 p<0.0001). The distribution of daughter centriole positions was not due to microscope
228 induced misalignment of the green and red channels: auto-fluorescent beads were
229 used to correct for microscope-induced offset between the channels (as in (Conduit et
230 al., 2015a)); and the data was taken from multiple nuclei/centrosome pairs, all of which
231 have different orientations with respect to the X-Y axes of the microscope. Moreover,
232 we observed a more random and non-Normal distribution of angles when imaging the

233 fluorescence recovery of two PCM proteins, Spd-2-GFP and RFP-Cnn, which are
234 expected to be closely aligned (Figure 1E,F; Figure S1C,D). Indeed, the positions of
235 the recovering RFP-Cnn signals relative to the recovering Spd-2-GFP signals were
236 much closer together with the mean distance between these signals ($0.099\mu\text{m}$) being
237 significantly shorter than the mean distance between the recovering Spd-2-GFP
238 (mother) and Sas-4-GFP (daughter) signals ($0.284\mu\text{m}$) (Figure 1G). We also repeated
239 the experiment using a green version of Sas-4 (Sas-4-GFP) and a different mother
240 centriole marker (Asl-mCherry) on a different microscope and again found that the
241 positions of daughter centriole assembly were not evenly distributed relative to the
242 future spindle axis (Figure S1E), that the angles from the future spindle axis were
243 Normally distributed around 0° (Figure S1F,G), that a much higher proportion of
244 daughter centrioles assembled within 90 degrees of the future spindle axis (Figure
245 S1H), and that the distance between the recovering signals was similar to that for the
246 Spd-2-GFP/Sas-4-mCherry data (Figure S1I). Collectively, this data shows that the
247 positioning of daughter centriole assembly in *Drosophila* syncytial embryos is non-
248 random with respect to cellular geometry.

249

250 The non-random position of daughter centriole assembly is dependent on centrosome 251 association with the nuclear envelope

252 In *Drosophila* syncytial embryos, the centrosomes are tightly associated with the
253 nuclear envelope via nuclear envelope associated Dynein (Robinson et al., 1999).
254 Thus, the observation that daughter centrioles form preferentially within 90° of the
255 future spindle axis also meant that they were preferentially positioned on the side of
256 the mother centriole facing the nuclear envelope. This raised the intriguing possibility
257 that the nuclear envelope might influence the position of daughter centriole assembly.
258 To test this, we wanted to examine the position of daughter centriole assembly in
259 centrosomes that had detached from the nuclear envelope. We knew that Threonine
260 1133 within the PCM protein Cnn is important for Cnn to oligomerise and form a PCM
261 scaffold (Feng et al., 2017) and our unpublished observations had shown that
262 substituting Threonine 1133 with Alanine partially perturbs scaffold formation and the
263 ability of centrosomes to remain attached to the nuclear envelope (see also Figure
264 2A). We therefore generated a stock co-expressing Sas-4-mCherry and a GFP-Cnn-

265 T1133A to analyse daughter centriole position in attached versus detached
266 centrosomes. The detached centrosomes in Cnn-T1133A mutants normally remain
267 relatively close to the nuclear envelope, do not fall into the embryo centre, and form a
268 spindle pole in during the following mitosis. Nevertheless, they often do not fully
269 migrate around the nucleus (Figure 2A). Thus, instead of using the line between paired
270 centrosomes as a reference point for the angle of daughter centriole assembly, we
271 used a line drawn between the mother centriole and the centre of the nucleus
272 (visualised due to the exclusion of fluorescence molecules), which we hereafter refer
273 to as the nuclear axis (Figure 2A,B).

274

275 We photobleached centrosomes in late mitosis and monitored the fluorescence
276 recovery during the following S-phase, noting which centrosomes had separated from
277 the nuclear envelope and which had not. Importantly, the daughter centrioles within
278 centrosomes that had remained attached to the nuclear envelope still displayed a
279 preference to assemble on the side of the mother facing the nuclear envelope (Figure
280 2C-F), showing that perturbation of the PCM via Cnn's T1133A mutation did not
281 indirectly affect daughter centriole positioning. In these attached centrosomes, the
282 estimated position of the daughter centrioles displayed a similar non-even distribution
283 to that observed in the analyses above for Spd-2-GFP;Sas-4-mCherry and Asl-
284 mCherry; Sas-4-GFP (compare Figures 1C, 2C and Figure S1E). The measured
285 angles of daughter centriole formation were normally distributed around 0° (Figure
286 2D,E) (passed all 4 Normality tests in Prism) and a Rose Plot graph highlighted how
287 66.3% (59 of 89) daughter centrioles were positioned within 90 degrees of 0° (Figure
288 2F) (Binomial Wilson/Brown test, $p < 0.01$). In contrast to the attached centrosomes,
289 the daughter centrioles within centrosomes detached from the nuclear envelope did
290 not display a preference to assemble on the side of the mother facing the nuclear
291 envelope (Figure 2G-J). The estimated position of these daughter centrioles was more
292 evenly spread around the mother centriole (Figure 2G) and the angles at which they
293 assembled relative to the nuclear axis were not normally distributed around 0° (Figure
294 2H,I) (Failed 3 of 4 Normality tests in Prism) and were not significantly different from
295 a random distribution (Chi-square=8.4, $df=11$, $p=0.68$). Moreover, there was no
296 preference for the centrioles to form within 90 degrees of the nuclear axis, with similar

297 numbers of daughter centrioles forming within 90 degrees (31/60) and more than 90
298 degrees (29/60) from the nuclear axis (Figure 2J) (Binomial Wilson/Brown test,
299 $p=0.90$).

300

301 It was possible that the perceived loss of preference for the daughter centriole to form
302 towards the nuclear axis in detached Cnn-T1133A centrosomes could have been an
303 indirect effect of defects in centriole orientation with respect to the imaging axis i.e.
304 detached centrosomes may tilt such that their daughter centrioles do not grow along
305 the X-Y imaging axis, causing increased noise and a possible randomising effect in
306 the data. We ruled this out in two different ways. First, we compared the frequency at
307 which GFP-Cnn-T1133A displayed a “central hole” at attached and detached
308 centrosomes. Cnn molecules surround the mother centriole such that, with sufficient
309 X-Y spatial resolution, a “hole” in the centre of the Cnn fluorescence signal can be
310 observed (e.g. top panels in Figure 3A, B). We reasoned that this central hole would
311 be observed only in centrosomes that had their mother centriole pointing normally
312 along the Z imaging axis. We imaged fixed embryos in S-phase expressing GFP-Cnn-
313 T1133A and Asl-mCherry (which labels only mother centrioles during S-phase) on a
314 Zeiss Airyscan 2 microscope, which increases X-Y spatial resolution to up to 120nm,
315 and quantified the frequency of “clear”, “partial”, or “no clear” central holes in attached
316 (Figure 3A) versus detached (Figure 3B) centrosomes. Out of a total of 112
317 centrosomes from 3 embryos, 83 were attached and 29 were detached. Of the 83
318 attached centrosomes, 38 (45.8%) displayed a clear central hole, 25 (30.1%)
319 displayed a partial central hole, and 20 (24.1%) displayed no clear central hole (Figure
320 3C). These percentages were similar in detached centrosomes. Of the 29 detached
321 centrosomes, 12 (41.4%) displayed a clear doughnut-like pattern, 9 (31.0%) displayed
322 a partial doughnut-like pattern, and 8 (27.6%) displayed no clear doughnut-like pattern
323 (Figure 3C). There was no significant difference between the categorisation of these
324 attached and detached centrosomes (Chi-square = 0.204, $df=2$, $p=0.903$), suggesting
325 that detached centrosomes are not mis-oriented compared to attached centrosomes.
326 To further support this finding, we used the previous Spd-2-GFP/Sas-4-mCherry
327 FRAP data (Figure 2C,G) to compare the median estimated distances between
328 mother and daughter centrioles in attached ($0.30\mu\text{m}$) versus detached ($0.33\mu\text{m}$)

329 centrosomes and found there was no significant difference (Figure 3D; Mann-Whitney,
330 $p=0.26$). The distance would in theory be shorter in detached centrosomes if they were
331 misoriented. Thus, the data suggests that mother centrioles within centrosomes that
332 have detached from the nuclear envelope remain aligned along the Z imaging axis.
333 We therefore conclude that, unlike in attached centrosomes, daughter centrioles within
334 detached centrosomes do not form preferentially towards the nuclear envelope and
335 that the nucleus somehow influences daughter centriole positioning.

336

337 The positioning of daughter centriole assembly is consistent through time

338 To estimate the position of daughter centrioles from our FRAP data, we had needed
339 to wait until the fluorescent signals had recovered sufficiently in order to take accurate
340 measurements, meaning that we could only assess daughter centriole positioning
341 during mid to late S-phase. We therefore wondered whether the initial steps of
342 daughter centriole formation occur with a positional preference, or whether they occur
343 in a random position with the daughter centriole rotating to face the nuclear envelope
344 later in S-phase. To address this, we performed live imaging of duplicating
345 centrosomes throughout S-phase using an Airyscan microscope that enabled us to
346 distinguish two mother and daughter foci of Sas-4-mCherry signal, with the mother
347 centriole localised in the centre of the Spd-2-GFP fluorescence (Figure 4A). Note that
348 the growing daughter centriole rapidly recruits excess Sas-4 (Conduit et al., 2015a)
349 and so appears brighter than the mother for the majority of S-phase, and that Spd-2-
350 GFP, like GFP-Cnn, surrounds the mother centriole and can display a central hole with
351 high enough spatial resolution (certain timepoints in Figure 4A; (Conduit et al., 2014)).
352 Exclusion of cytoplasmic fluorescence can also be used to assess the position of the
353 nuclear envelope (data not shown), which is indicated in blue in Figure 4A (note that
354 centrosomes can migrate over the nucleus, explaining why the paired centrosome in
355 timepoint 1 overlaps the nuclear region).

356

357 We followed 72 centrosomes for at least 6 timepoints (~5 minutes) and collated the
358 data. Note that for most centrosomes, the mother and daughter centrioles within a pair
359 were not resolvable for all 6 timepoints and so the number of measurements per
360 timepoint varied between timepoints. We found that daughter centrioles had a strong

361 preference to assemble on the side of the mother facing the nuclear envelope from
362 the earliest stage of S-phase that the daughter centrioles were visible (timepoint 1,
363 Figure 4B). Moreover, this preference remained throughout the 6 timepoints (Figure
364 4B). Indeed, we found that daughter centriole positioning relative to the nuclear axis
365 remained quite stable over time. The median angle deviation between timepoints was
366 21.5° , which is much lower than the median angle deviation expected were the
367 daughter centrioles to be positioned randomly at each timepoint ($\sim 90^\circ$). Indeed, the
368 distribution of deviation angles was significantly different from the distribution of
369 random number data (Figure 4C; $p < 0.0001$ Kolmogorov-Smirnov test). Collectively,
370 this data shows that daughter centriole assembly is initiated preferentially on the side
371 of the mother facing the nuclear envelope and that this positioning remains relatively
372 stable throughout daughter centriole assembly.

373

374 **Discussion**

375 We have shown that during the mitotic nuclear cycles in *Drosophila* syncytial embryos
376 daughter centrioles preferentially assemble on the side of the mother centriole facing
377 the nuclear envelope. This preferential positioning is lost when centrosomes become
378 detached from the nuclear envelope, raising the intriguing possibility that crosstalk
379 between nuclear-envelope-related factors and the centriole duplication machinery
380 may help to instruct centriole duplication. It remains to be seen whether an attachment
381 to the nuclear envelope influences centriole duplication in other cell types, but the
382 centrosome is not always attached to the nuclear envelope in all cell types. It remains
383 possible, however, that other cellular structures could be involved in these cells, or
384 that daughter centriole positioning is random, relying on stochastic processes.

385

386 We used a Cnn point mutant (Cnn-T1133A) to show that daughter centrioles within
387 detached centrosomes lose their preferential positioning towards the nuclear
388 envelope. This mutation has a relatively subtle effect on PCM assembly and stability,
389 while being sufficient to cause a fraction of centrosomes to detach from the nuclear
390 envelope. We predict that this detachment is stochastic and occurs because fewer
391 microtubules can be organised at centrosomes with reduced PCM. Thus, there is a
392 chance that some centrosomes will detach from the nuclear envelope. PCM levels are
393 not low enough, however, to cause Cnn-T1133A centrosomes to ‘rocket’ around the
394 embryo, unlike centrosomes completely lacking Cnn (Lucas and Raff, 2007), and we
395 do not see any obvious effect on centriole structure or duplication. We therefore
396 consider that the loss of preferential daughter centriole positioning in detached Cnn-
397 T1133A centrosomes is not due to PCM instability *per se*, especially as the daughter
398 centrioles within attached Cnn-T1133A centrosomes still retain a biased position
399 towards the nuclear envelope. Although this bias (66%) appears to be lower than that
400 recorded when looking at “wild-type” centrosomes (78.5% when using Spd-2-GFP and
401 Sas-4-mCherry; 72.9% when using Asl-mCherry and Sas-4-GFP), we believe this is
402 due to a lower accuracy of estimating mother centriole position when using Cnn-
403 T1133A as opposed to using Spd-2 and Asl. This is because Spd-2 and Asl
404 incorporate very close to the wall of the mother centriole, while Cnn incorporates into
405 a broader area (Conduit et al., 2014), meaning that the recovering fluorescent signals

406 of Spd-2 and Asl better predict mother centriole position. It would be satisfying to
407 repeat the experiment with a mutation that perturbs centrosome attachment to the
408 nuclear envelope without affecting centrosome structure at all, such as mutations in
409 the LINC complex, but these experiments would be technically challenging due to the
410 complex genetics and possible maternal effects of LINC mutants.

411

412 Further work is needed to understand the molecular basis for the positional bias, as
413 well as understanding its importance, if any. We do not observe any obvious centriole
414 duplication defects in Cnn-T1133A centrosomes that have detached from the nuclear
415 envelope, indicating that the influence of the nuclear envelope on centriole duplication
416 is not essential to ensure the production of a single daughter centriole, but we have
417 not examined this extensively and it could still make the process more robust.

418

419 **Opening Up**

420 A major outstanding question is how PLK4 symmetry breaking is achieved to ensure
421 that only one daughter centriole is formed on the side of the radially symmetric mother
422 centriole (Yamamoto and Kitagawa, 2021). It is known that the PLK4 ring-to-dot
423 transition requires proteasome activity (Ohta et al., 2014), Plk4 activity (Ohta et al.,
424 2018; Park et al., 2019), and phosphorylation of PLK4's cryptic polo box (Park et al.,
425 2019), suggesting that the auto-catalytic self-destructive properties of PLK4 could
426 regulate the transition (Leda et al., 2018; Park et al., 2019; Takao et al., 2019;
427 Yamamoto and Kitagawa, 2021, 2019). Indeed, computer modelling suggests that
428 PLK4 symmetry breaking can be initiated by the self-organisational properties of PLK4
429 (Leda et al., 2018; Takao et al., 2019). An initial stochastic break in symmetry could
430 then be enhanced by the binding of STIL (Leda et al., 2018; Takao et al., 2019), which
431 both stimulates PLK4 activity (Moyer et al., 2015) and protects Plk4 from degradation
432 (Arquint et al., 2015; Ohta et al., 2014). The different computer simulations place a
433 difference emphasis on the role of STIL binding (Leda et al., 2018; Takao et al., 2019),
434 but both agree that this is a critical step in completing the ring-to-dot transition. It is
435 intriguing that STIL is able to bind to only a single site on the mother centriole even
436 when PLK4 remains as a ring after proteasome inhibition (Ohta et al., 2014),
437 suggesting that STIL recruitment to a single site within the ring of Plk4 could even be

438 the initial trigger for symmetry breaking in certain circumstances. In *Drosophila* S2
439 cells, the first observed break in symmetry is the recruitment of the STIL homologue,
440 Ana2, to a single spot on the mother centriole (Dzhindzhev et al., 2017).

441

442 Is there a link between PLK4, Ana2 and the nuclear envelope? In various cell types,
443 including *Drosophila* syncytial embryos, the centrosomes are tightly associated with
444 the nuclear envelope via interactions between the microtubules they organise and
445 nuclear-envelope-associated Dynein (Agircan et al., 2014; Bolhy et al., 2011;
446 Raaijmakers et al., 2012; Robinson et al., 1999; Splinter et al., 2010). From our
447 observations, we speculate that molecules associated with the nuclear envelope or
448 concentrated within the local environment between centrosomes and the nuclear
449 envelope may help determine the position of centriole duplication proteins in
450 *Drosophila* syncytial embryos. These putative molecules may help stabilise Plk4 or
451 recruit Ana2, or both. This could relate to the asymmetry in centrosomal microtubules,
452 with differences in the ability of the microtubules connecting the centrosomes to the
453 nuclear envelope and the microtubules extending out into the cytosol to concentrate
454 PLK4 and Ana2. Alternatively, perhaps proteins associated with the nuclear envelope
455 can transiently bind Plk4 or Ana2 and thus increase their local concentration in the
456 region between the mother centriole and nuclear envelope. Ana2 directly interacts with
457 a conserved member of the Dynein complex, Cut-up (Ctp), which is a form of Dynein
458 Light Chain in *Drosophila* (Slevin et al., 2014; Wang et al., 2011). Although the precise
459 function of the Ana2-Ctp interaction remains unclear, it appears to help mediate Ana2
460 tetramerisation (Slevin et al., 2014), and Ana2 tetramerisation is important for centriole
461 assembly (Cottee et al., 2015). Thus, while Ctp does not appear to be essential for
462 centriole duplication (Wang et al., 2011), any Ctp molecules released from the nuclear
463 associated Dynein complexes would be ideally positioned to bind to Ana2 and promote
464 daughter centriole assembly on the side of the mother centriole facing the nuclear
465 envelope.

466

467 It will also be interesting to see whether positional bias occurs in other systems.
468 Intriguingly, LRRCC1 has recently been shown to localise asymmetrically within the
469 lumen of human centrioles with the position of procentriole assembly being non-

470 random with respect to this asymmetric mark (Gaudin et al., 2021). Thus, although the
471 molecular nature may vary, it's possible that a non-random positional preference in
472 daughter centriole assembly is an important conserved feature of centriole duplication.

473

474

475 **Acknowledgements**

476 This work was supported by a BBSRC New Investigator Award (BB/P019188/1), a
477 Wellcome Trust and Royal Society Sir Henry Dale Fellowship (105653/Z/14/Z) and an
478 IdEx Université de Paris ANR-18-IDEX-0001 awarded to PTC. We thank Jordan Raff
479 for fly lines and the use of his spinning disk microscope. We thank Alan Wainman for
480 help with live Airyscan imaging. We thank Corinne Tovey for critical reading of the
481 manuscript. The work benefited from use of the imaging facility at the Stem Cell
482 Institute, University of Cambridge, the Micron imaging facility at the University of
483 Oxford, and the imaging facility at the Institut Jacques Monod, Université de Paris.
484 NHJC made the initial observation of positional preference by performing and
485 analysing dual FRAP experiments with Spd-2-GFP / Sas-4-mCherry and Spd-2-GFP
486 / RFP-Cnn, devised the formula to calculate angles, and performed and analysed the
487 live Airyscan experiments. IB collected additional data for the dual FRAP experiments
488 with Spd-2-GFP and Sas-4-mCherry and measured distances between centrioles in
489 detached versus attached centrioles. PTC designed the study, performed all other
490 experiments and analysis, and wrote the manuscript. The authors declare no financial
491 or non-financial competing interests.

492

493 **Figure Legends**

494

495 **Figure 1**

496 **Analysis of dual-colour FRAP data reveals that the site of daughter centriole**
497 **assembly is non-random. (A)** Confocal images show a centrosome within an embryo
498 expressing Spd-2-GFP (green) and Sas-4-mCherry (magenta) prior to photobleaching
499 (left), immediately after photobleaching (centre), and after fluorescence recovery
500 (right). The diagrams below are cartoon representations of how the proteins behave
501 before and after photobleaching. Note that the recovering Sas-4-mCherry signal
502 (daughter centriole) is offset from the centre of the recovering Spd-2-GFP signal
503 (mother centriole). **(B)** Confocal image shows a pair of centrosomes (top unbleached,
504 bottom recovering from bleaching) on opposite sides of the nuclear envelope (mid-late
505 S-phase). The nuclear envelope and how angles from the future spindle axis are
506 calculated are indicated. **(C)** Graph displays the estimated positions of daughter
507 centrioles (magenta circles) relative to the estimated position of their respective
508 mother centrioles (position 0,0 on the graph) and the future spindle axis (positive y-
509 axis) obtained from Spd-2-GFP (mother) Sas-4-mCherry (daughter) data. **(D)** Rose
510 plot representing the angle at which daughter centrioles (marked by Sas-4-mCherry)
511 form in relation to the future spindle axis (0°). Each segment corresponds to a single
512 duplication event. Blue and red segments indicate daughter centriole assembly
513 occurring less than or more than 90° from the future spindle axis, respectively. **(E)**
514 Graph displays the positions of the centre of recovering RFP-Cnn signal relative to
515 recovering Spd-2-GFP signal (position 0,0 on the graph) and the future spindle axis
516 (positive y-axis) obtained from the control Spd-2-GFP (mother) RFP-Cnn (mother)
517 data. **(F)** Rose plot (as in (D)) representing the angle relative to the future spindle axis
518 (0°) formed by a line running between the recovering Spd-2-GFP and RFP-Cnn
519 signals. **(G)** Graph showing the distance between the centre of the recovering Spd-2-
520 GFP signal (mother centriole) and the recovering Sas-4-mCherry signal (daughter
521 centriole, magenta) or the recovering RFP-Cnn signal (mother centriole). The datasets
522 were compared using a Mann-Whitney test.

523

524 **Figure 2**

525 **The site of daughter centriole assembly is random in centrosomes that have**
526 **detached from the nuclear envelope. (A,B)** Confocal image (A) and cartoon
527 representation (B) show a pair of centrosomes in S-phase within an embryo
528 expressing GFP-Cnn-T1133A (grayscale). Note that one centrosome is attached to
529 and one centrosome is detached from the nuclear envelope. Cartoon in (B) indicates
530 how the angles of daughter centriole assembly from the nuclear axis were measured.
531 **(C-J)** Graphs display results from analysing the estimated position of daughter
532 centrioles relative to the estimated position of their respective mother centrioles
533 (position 0,0 on the graph) and the nuclear axis (positive y-axis) in centrosomes that
534 have either remained attached to (C-F) or that have detached from (D-J) the nuclear
535 envelope within embryos expressing GFP-Cnn-T1133A and Sas-4-mCherry.
536 Estimated positions of the daughter centrioles were determined from analysing the
537 centre of fluorescence recovery of GFP-Cnn-T1133A (mother) and Sas-4-mCherry
538 (daughter). Graphs in (C) and (G) show the estimated positions of the daughter
539 centrioles; (D) and (H) are frequency distributions of the angles at which daughter
540 centriole form in relation to the nuclear axis (0°); (E) and (I) are normal QQ plot showing
541 that the angles in (E), but not in (I), conform well to a Normal distribution; Rose plots
542 in (F) and (J) represent the angle at which daughter centrioles form in relation to the
543 mother centriole and the nuclear axis (0°). Each segment corresponds to a single
544 duplication event. Blue and red segments indicate daughter centriole assembly
545 occurring less than or more than 90° from the nuclear axis, respectively.

546

547 **Figure 3**

548 **Cnn-T1133A centrosomes that have detached from the nuclear envelope remain**
549 **correctly oriented with respect to the imaging axis. (A,B)** Airyscan images of
550 centrosomes that are either attached to (A) or detached from (B) the nuclear envelope
551 within embryos expressing GFP-Cnn-T1133A and Sas-4-mCherry in a *cnn* null mutant
552 background. Examples with a clear central hole (top panels), a partial central hole
553 (middle panels), and a no clear central hole (bottom panels) are shown. **(C)** Graph
554 shows the percentage of each centrosome type in either attached or detached
555 centrosomes, as indicated. Datasets were compared using a Chi-squared contingency
556 analysis. **(D)** Graph shows the distances between the estimated positions of mother

557 and daughter centrioles from the Spd-2-GFP/Sas-4-mCherry FRAP data in either
558 attached or detached centrosomes, as indicated. The datasets were compared using
559 a Mann-Whitney test.

560

561 **Figure 4**

562 **Daughter centrioles initially form preferentially towards the nuclear envelope**

563 **and retain a stable position throughout S-phase. (A)** Airyscan images of a

564 centrosome in an embryo expressing Spd-2-GFP (green) and Sas-4-mCherry

565 (magenta) progressing through S-phase. Approximate times after centrosome splitting

566 are indicated – images were collected approximately every minute. The position of the

567 nuclear envelope (as determined by the exclusion of fluorescence from the nucleus)

568 is indicated by the dotted blue line. The Sas-4-mCherry signals for mother (m) and

569 daughter (d) centrioles are also indicated. (B) Rose plot graphs display the angle at

570 which daughter centrioles form in relation to the mother centriole and the nuclear axis

571 (0°) as calculated from time-lapse Airyscan images that followed centrosomes

572 throughout S-phase. Each segment corresponds to a single duplication event. Blue

573 and red segments indicate daughter centriole assembly occurring less than or more

574 than 90° from the nuclear axis, respectively. Each rose plot corresponds to a given

575 timepoint, with timepoint 1 occurring ~ 1 minute after centrosome splitting and there

576 being a ~ 1 -minute gap between timepoints. The numbers of events for each timepoint

577 are indicated; this varies due to the varying ability to resolve the two centrioles through

578 time. (C) Graph shows the change in the angle of the daughter centriole (angle

579 deviation) with respect to the mother centriole and the nuclear axis that occurred

580 between timepoints from real data (left dataset) or randomly generated angles (right

581 dataset). Each point on the graph represents an individual angle deviation. The

582 median and 95% CIs are shown. The p value indicates that the two datasets have a

583 different distribution (Kolmogorov-Smirnov test).

584

585 **Materials and methods**

586 **Contact for Reagent and Resource Sharing**

587 Further information and requests for resources and reagents should be directed to and
588 will be fulfilled by the Lead Contact, Paul Conduit (paul.conduit@ijm.fr).

589

590 **Experimental Model and Subject Details**

591 All fly strains were maintained at 18 or 25°C on Iberian fly food made from dry active
592 yeast, agar, and organic pasta flour, supplemented with nipagin, propionic acid,
593 pen/strep and food colouring.

594

595 **Methods**

596 *Drosophila melanogaster* stocks

597 The following fluorescent alleles were used in this study: pUbq-Spd-2-GFP (Dix and
598 Raff, 2007), eSas-4-mCherry (endogenous promoter) (Conduit et al., 2015a), pUbq-
599 RFP-Cnn (Conduit et al., 2010), eSas-4-GFP (endogenous promoter) (Novak et al.,
600 2014), eAsl-mCherry (endogenous promoter) (Conduit et al., 2015a), pUbq-GFP-Cnn-
601 T1133A (this study). To make the pUbq-GFP-Cnn-T1133A allele, we used
602 QuikChange (Agilent) to introduce the T1133A mutation into Cnn within a pDONR
603 vector and used Gateway cloning (ThermoFisher) to transfer it into a pUbq-GFP vector
604 containing a miniwhite marker. This construct was injected by BestGene in order to
605 generate transgenic lines.

606

607 For performing FRAP experiments we used fly lines expressing either: two copies of
608 pUbq-Spd-2-GFP and two copies eSas-4-mCherry in a *sas-4* null background (*sas-*
609 *4^{l(3)2214}/Df(3R)BSC221*); two copies of pUbq-Spd-2-GFP and one copy of RFP-Cnn in
610 a *cnn^{f04547}/cnn^{HK21}* mutant background; two copies of eSas-4-GFP and two copies of
611 eAsl-mCherry in a *sas-4* null background (*sas-4^{l(3)2214}/Df(3R)BSC221*); or one copy of
612 pUbq-GFP-Cnn-T1133A and two copies eSas-4-mCherry in a *sas-4* null background
613 (*sas-4^{l(3)2214}/Df(3R)BSC221*). For the live Airyscan imaging, we used flies expressing
614 two copies of pUbq-Spd-2-GFP and two copies eSas-4-mCherry in a *sas-4* null
615 background (*sas-4^{l(3)2214}/Df(3R)BSC221*). For the fixed Airyscan imaging, we used

616 flies expressing one copy of pUbq-GFP-Cnn-T1133A and two copies eAsl-mCherry in
617 an *asl*/null mutant background (*asl*^{mecd} (Blachon et al., 2008)).

618

619 Fixed and live cell imaging

620 For live dual FRAP experiments, 0.5µm thick confocal sections were collected from
621 living syncytial embryos in nuclear cycle 11 or 12 at ~21°C on either a Perkin Elmer
622 ERS Spinning Disk confocal system mounted on a Zeiss Axiovert microscope using a
623 63X/1.4NA Oil objective, or an Andor Revolution Spinning Disk confocal system
624 mounted on a Nikon Ti inverted microscope coupled to an Andor iXon camera using
625 a Plan-Apochromat 60X/1.4NA Oil objective. Focused 488nm and 561nm lasers were
626 used to photobleach the GFP and mCherry/RFP signals, respectively. For live
627 Airyscan imaging, 0.2 µm thick sections were collected from living embryos in nuclear
628 cycle 12 or 13 on an inverted Zeiss 880 microscope fitted with an Airyscan detector
629 at 21°C and a Plan-Apochromat 63x/1.4NA oil lens using 488-nm argon and 561-nm
630 diode lasers. Images were collected approximately every 1 min with a zoom value of
631 23.3 pixels/µm. Focus was readjusted between the 1-min intervals. Images were Airy-
632 processed in 3D with a strength value of “auto” (~6) or 6.5. For fixed Airyscan imaging,
633 0.2 µm thick sections were collected from methanol fixed embryos in nuclear cycle 11
634 or 12 on an inverted Zeiss LSM980 microscope fitted with an Airyscan2 detector
635 at 21°C and a Plan-Apochromat 63x/1.4NA oil lens using 488-nm argon and 561-nm
636 diode lasers. When measuring centriole positions, images from the different colour
637 channels were registered with alignment parameters obtained from calibration
638 measurements with 0.2 µm diameter TetraSpeck beads (Life Technologies). The
639 centroids of each fluorescent signal were calculated in ImageJ using the “centre of
640 mass” analysis tool. The number of pixels for the images was first increased such that
641 each real pixel was made of 5x5 sub-pixels. This increases the location accuracy for
642 the centroid of the fluorescence signal.

643

644 Quantification and Statistical Analysis

645 Data was processed in Microsoft Excel. Graph production was performed using either
646 Microsoft Excel (rose plots) or GraphPad Prism (all other graphs) and statistical
647 analysis was performed using GraphPad Prism. N numbers and statistical tests used

648 for each experiment are indicated within the main text or Figure Legends. The
649 following Normality tests were carried out in Prism to analyse the frequency
650 distributions of angles: Anderson-Darling test, D'Agostino & Pearson test, Shapiro-
651 Wilk test, Kolmogorov-Smirnov test.

652

653

654

655 **References**

656
657

- 658 Agircan FG, Schiebel E, Mardin BR. 2014. Separate to operate: control of
659 centrosome positioning and separation. *Philosophical Transactions Royal Soc B*
660 *Biological Sci* 369:20130461–20130461. doi:10.1098/rstb.2013.0461
- 661 Anderhub SJ, Krämer A, Maier B. 2012. Centrosome amplification in tumorigenesis.
662 *Cancer Lett* 322:8–17. doi:10.1016/j.canlet.2012.02.006
- 663 Arquint C, Gabryjonczyk A-M, Imseng S, Böhm R, Sauer E, Hiller S, Nigg EA, Maier
664 T. 2015. STIL binding to Polo-box 3 of PLK4 regulates centriole duplication. *Elife*
665 4:e07888. doi:10.7554/elife.07888
- 666 Arquint C, Nigg EA. 2016. The PLK4–STIL–SAS-6 module at the core of centriole
667 duplication. *Biochem Soc T* 44:1253–1263. doi:10.1042/bst20160116
- 668 Banterle N, Gönczy P. 2017. Centriole Biogenesis: From Identifying the Characters
669 to Understanding the Plot. *Annu Rev Cell Dev Bi* 33:23–49. doi:10.1146/annurev-
670 cellbio-100616-060454
- 671 Basto R, Brunk K, Vinadogrova T, Peel N, Franz A, Khodjakov A, Raff JW. 2008.
672 Centrosome amplification can initiate tumorigenesis in flies. *Cell* 133:1032–1042.
673 doi:10.1016/j.cell.2008.05.039
- 674 Basto R, Lau J, Vinogradova T, Gardiol A, Woods CG, Khodjakov A, Raff JW. 2006.
675 Flies without centrioles. *Cell* 125:1375–1386. doi:10.1016/j.cell.2006.05.025
- 676 Bettencourt-Dias M, Rodrigues-Martins A, Carpenter L, Riparbelli M, Lehmann L,
677 Gatt MK, Carmo N, Balloux F, Callaini G, Glover DM. 2005. SAK/PLK4 is required
678 for centriole duplication and flagella development. *Curr Biol* 15:2199–2207.
679 doi:10.1016/j.cub.2005.11.042
- 680 Blachon S, Gopalakrishnan J, Omori Y, Polyanovsky A, Church A, Nicastro D,
681 Malicki J, Avidor-Reiss T. 2008. Drosophila asterless and vertebrate Cep152 Are
682 orthologs essential for centriole duplication. *Genetics* 180:2081–2094.
683 doi:10.1534/genetics.108.095141
- 684 Bolhy S, Bouhlef I, Dultz E, Nayak T, Zuccolo M, Gatti X, Vallee R, Ellenberg J, Doye
685 V. 2011. A Nup133-dependent NPC-anchored network tethers centrosomes to the
686 nuclear envelope in prophase. *J Cell Biology* 192:855–871.
687 doi:10.1083/jcb.201007118
- 688 Brownlee CW, Klebba JE, Buster DW, Rogers GC. 2011. The Protein Phosphatase
689 2A regulatory subunit Twins stabilizes Plk4 to induce centriole amplification. *J Cell*
690 *Biology* 195:231–243. doi:10.1083/jcb.201107086

- 691 Cizmecioglu O, Arnold M, Bahtz R, Settele F, Ehret L, Haselmann-Weiß U, Antony
692 C, Hoffmann I. 2010. Cep152 acts as a scaffold for recruitment of Plk4 and CPAP
693 to the centrosome. *J Cell Biology* 191:731–739. doi:10.1083/jcb.201007107
- 694 Conduit PT, Brunk K, Dobbelaere J, Dix CI, Lucas EP, Raff JW. 2010. Centrioles
695 regulate centrosome size by controlling the rate of Cnn incorporation into the
696 PCM. *Curr Biol* 20:2178–2186. doi:10.1016/j.cub.2010.11.011
- 697 Conduit PT, Richens JH, Wainman A, Holder J, Vicente CC, Pratt MB, Dix CI, Novak
698 ZA, Dobbie IM, Schermelleh L, Raff JW. 2014. A molecular mechanism of mitotic
699 centrosome assembly in *Drosophila*. *Elife* 3:2987. doi:10.7554/elife.03399
- 700 Conduit PT, Wainman A, Novak ZA, Weil TT, Raff JW. 2015a. Re-examining the role
701 of *Drosophila* Sas-4 in centrosome assembly using two-colour-3D-SIM FRAP.
702 *Elife* 4:e08483. doi:10.7554/elife.08483
- 703 Conduit PT, Wainman A, Raff JW. 2015b. Centrosome function and assembly in
704 animal cells. *Nat Rev Mol Cell Bio* 16:611–624. doi:10.1038/nrm4062
- 705 Cottee MA, Muschalik N, Johnson S, Leveson J, Raff JW, Lea SM. 2015. The homo-
706 oligomerisation of both Sas-6 and Ana2 is required for efficient centriole assembly
707 in flies. *Elife* 4:e07236. doi:10.7554/elife.07236
- 708 Cunha-Ferreira I, Bento I, Pimenta-Marques A, Jana SC, Lince-Faria M, Duarte P,
709 Borrego-Pinto J, Gilberto S, Amado T, Brito D, Rodrigues-Martins A, Debski J,
710 Dzhindzhev N, Bettencourt-Dias M. 2013. Regulation of autophosphorylation
711 controls PLK4 self-destruction and centriole number. *Curr Biol* 23:2245–2254.
712 doi:10.1016/j.cub.2013.09.037
- 713 Cunha-Ferreira I, Rodrigues-Martins A, Bento I, Riparbelli M, Zhang W, Laue E,
714 Callaini G, Glover DM, Bettencourt-Dias M. 2009. The SCF/Slimb ubiquitin ligase
715 limits centrosome amplification through degradation of SAK/PLK4. *Curr Biol* 19:43
716 49. doi:10.1016/j.cub.2008.11.037
- 717 Dammermann A, Müller-Reichert T, Pelletier L, Habermann B, Desai A, Oegema K.
718 2004. Centriole Assembly Requires Both Centriolar and Pericentriolar Material
719 Proteins. *Dev Cell* 7:815–829. doi:10.1016/j.devcel.2004.10.015
- 720 Delattre M, Canard C, Gönczy P. 2006. Sequential protein recruitment in *C. elegans*
721 centriole formation. *Curr Biol* 16:1844–1849. doi:10.1016/j.cub.2006.07.059
- 722 Denu RA, Zasadil LM, Kanugh C, Laffin J, Weaver BA, Burkard ME. 2016.
723 Centrosome amplification induces high grade features and is prognostic of worse
724 outcomes in breast cancer. *Bmc Cancer* 16:47. doi:10.1186/s12885-016-2083-x
- 725 Dix CI, Raff JW. 2007. *Drosophila* Spd-2 Recruits PCM to the Sperm Centriole, but
726 Is Dispensable for Centriole Duplication. *Curr Biol* 17:1759–1764.
727 doi:10.1016/j.cub.2007.08.065

- 728 Dzhindzhev NS, Tzolovsky G, Lipinski Z, Abdelaziz M, Debski J, Dadlez M, Glover
729 DM. 2017. Two-step phosphorylation of Ana2 by Plk4 is required for the
730 sequential loading of Ana2 and Sas6 to initiate procentriole formation. *Open Biol*
731 7:170247. doi:10.1098/rsob.170247
- 732 Dzhindzhev NS, Yu QD, Weiskopf K, Tzolovsky G, Cunha-Ferreira I, Riparbelli M,
733 Rodrigues-Martins A, Bettencourt-Dias M, Callaini G, Glover DM. 2010. Asterless
734 is a scaffold for the onset of centriole assembly. *Nature* 467:714 718.
735 doi:10.1038/nature09445
- 736 Feng Z, Caballe A, Wainman A, Johnson S, Haensele AFM, Cottee MA, Conduit PT,
737 Lea SM, Raff JW. 2017. Structural Basis for Mitotic Centrosome Assembly in
738 Flies. *Cell* 169:1078 1089.e13. doi:10.1016/j.cell.2017.05.030
- 739 Firat-Karalar EN, Stearns T. 2014. The centriole duplication cycle. *Philosophical*
740 *Transactions Royal Soc B Biological Sci* 369:20130460–20130460.
741 doi:10.1098/rstb.2013.0460
- 742 Fu J, Hagan IM, Glover DM. 2015. The Centrosome and Its Duplication Cycle. *Csh*
743 *Perspect Biol* 7:a015800. doi:10.1101/cshperspect.a015800
- 744 Ganem N, Godinho S, Pellman D. 2009. A mechanism linking extra centrosomes to
745 chromosomal instability. *Nature* 460. doi:10.1038/nature08136
- 746 Gaudin N, Gil PM, Boumendjel M, Ershov D, Pioche-Durieu C, Bouix M, Delobelle Q,
747 Maniscalco L, Phan TBN, Heyer V, Reina-San-Martin B, Azimzadeh J. 2021.
748 Evolutionary conservation of centriole rotational asymmetry in the human
749 centrosome. *Biorxiv* 2021.07.21.453218. doi:10.1101/2021.07.21.453218
- 750 Godinho SA, Pellman D. 2014. Causes and consequences of centrosome
751 abnormalities in cancer. *Philosophical Transactions Royal Soc B Biological Sci*
752 369:20130467–20130467. doi:10.1098/rstb.2013.0467
- 753 Godinho SA, Picone R, Burute M, Dagher R, Su Y, Leung CT, Polyak K, Brugge JS,
754 Théry M, Pellman D. 2014. Oncogene-like induction of cellular invasion from
755 centrosome amplification. *Nature* 510:167 171. doi:10.1038/nature13277
- 756 Gouveia SM, Zitouni S, Kong D, Duarte P, Gomes BF, Sousa AL, Tranfield EM,
757 Hyman A, Loncarek J, Bettencourt-Dias M. 2018. PLK4 is a microtubule-
758 associated protein that self assembles promoting de novo MTOC formation. *J Cell*
759 *Sci* 132:jcs.219501. doi:10.1242/jcs.219501
- 760 Guderian G, Westendorf J, Uldschmid A, Nigg EA. 2010. Plk4 trans-
761 autophosphorylation regulates centriole number by controlling betaTrCP-mediated
762 degradation. *J Cell Sci* 123:2163 2169. doi:10.1242/jcs.068502
- 763 Habedanck R, Stierhof Y-D, Wilkinson CJ, Nigg EA. 2005. The Polo kinase Plk4
764 functions in centriole duplication. *Nat Cell Biol* 7:1140 1146. doi:10.1038/ncb1320

765 Hatch EM, Kulukian A, Holland AJ, Cleveland DW, Stearns T. 2010. Cep152
766 interacts with Plk4 and is required for centriole duplication. *J Cell Biology*
767 191:721–729. doi:10.1083/jcb.201006049

768 Holland AJ, Lan W, Niessen S, Hoover H, Cleveland DW. 2010. Polo-like kinase 4
769 kinase activity limits centrosome overduplication by autoregulating its own
770 stability. *J Cell Biology* 188:191–198. doi:10.1083/jcb.200911102

771 Kim T-S, Park J-E, Shukla A, Choi S, Murugan RN, Lee JH, Ahn M, Rhee K, Bang
772 JK, Kim BY, Loncarek J, Erikson RL, Lee KS. 2013. Hierarchical recruitment of
773 Plk4 and regulation of centriole biogenesis by two centrosomal scaffolds, Cep192
774 and Cep152. *Proc National Acad Sci* 110:E4849–E4857.
775 doi:10.1073/pnas.1319656110

776 Klebba JE, Buster DW, Nguyen AL, Swatkoski S, Gucek M, Rusan NM, Rogers GC.
777 2013. Polo-like Kinase 4 Autodeconstructs by Generating Its Slimb-Binding
778 Phosphodegron. *Curr Biol* 23:2255–2261. doi:10.1016/j.cub.2013.09.019

779 Kleylein-Sohn J, Westendorf J, Clech ML, Habedanck R, Stierhof Y-D, Nigg EA.
780 2007. Plk4-induced centriole biogenesis in human cells. *Dev Cell* 13:190–202.
781 doi:10.1016/j.devcel.2007.07.002

782 Leda M, Holland AJ, Goryachev AB. 2018. Autoamplification and competition drive
783 symmetry breaking: Initiation of centriole duplication by the PLK4-STIL network.
784 *Science* 361:222–235. doi:10.1126/science.1257833

785 Leidel S, Delattre M, Cerutti L, Baumer K, Gönczy P. 2005. SAS-6 defines a protein
786 family required for centrosome duplication in *C. elegans* and in human cells. *Nat*
787 *Cell Biol* 7:115–125. doi:10.1038/ncb1220

788 Leidel S, Gönczy P. 2003. SAS-4 Is Essential for Centrosome Duplication in *C.*
789 *elegans* and Is Recruited to Daughter Centrioles Once per Cell Cycle. *Dev Cell*
790 4:431–439. doi:10.1016/s1534-5807(03)00062-5

791 Loncarek J, Bettencourt-Dias M. 2018. Building the right centriole for each cell type.
792 *J Cell Biol* 217:823–835. doi:10.1083/jcb.201704093

793 Lucas EP, Raff JW. 2007. Maintaining the proper connection between the centrioles
794 and the pericentriolar matrix requires *Drosophila* Centrosomin. *J Cell Biology*
795 178:725–732. doi:10.1083/jcb.200704081

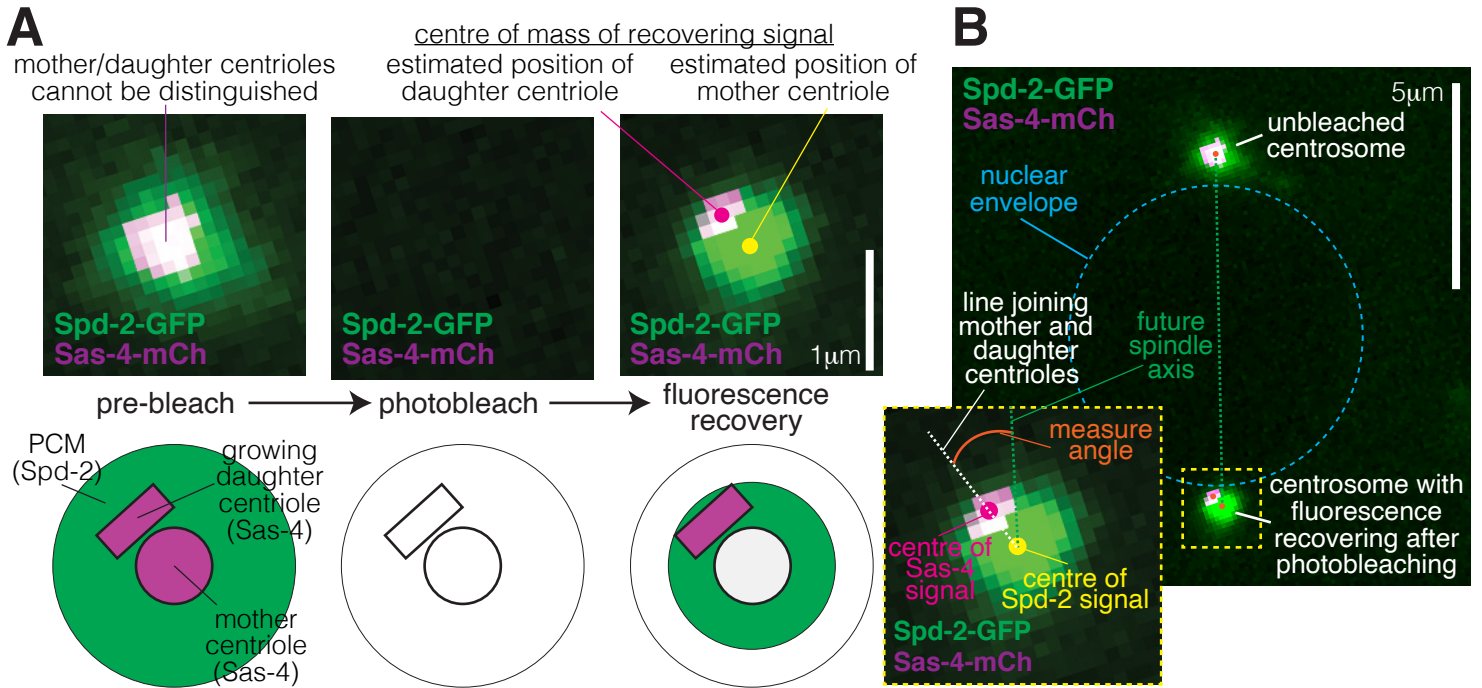
796 Mittal K, Kaur J, Jaczko M, Wei G, Toss MS, Rakha EA, Janssen EAM, Søiland H,
797 Kucuk O, Reid MD, Gupta MV, Aneja R. 2021. Centrosome amplification: a
798 quantifiable cancer cell trait with prognostic value in solid malignancies. *Cancer*
799 *Metast Rev* 40:319–339. doi:10.1007/s10555-020-09937-z

- 800 Moyer TC, Clutario KM, Lambrus BG, Daggubati V, Holland AJ. 2015. Binding of
801 STIL to Plk4 activates kinase activity to promote centriole assembly. *J Cell*
802 *Biology* 209:863–878. doi:10.1083/jcb.201502088
- 803 Nigg EA, Holland AJ. 2018. Once and only once: mechanisms of centriole
804 duplication and their deregulation in disease. *Nat Rev Mol Cell Bio* 19:297–312.
805 doi:10.1038/nrm.2017.127
- 806 Novak ZA, Conduit PT, Wainman A, Raff JW. 2014. Asterless licenses daughter
807 centrioles to duplicate for the first time in *Drosophila* embryos. *Curr Biol* 24:1276
808 1282. doi:10.1016/j.cub.2014.04.023
- 809 O’Connell KF, Caron C, Kopish KR, Hurd DD, Kempfues KJ, Li Y, White JG. 2001.
810 The *C. elegans* zyg-1 Gene Encodes a Regulator of Centrosome Duplication with
811 Distinct Maternal and Paternal Roles in the Embryo. *Cell* 105:547–558.
812 doi:10.1016/s0092-8674(01)00338-5
- 813 Ohta M, Ashikawa T, Nozaki Y, Kozuka-Hata H, Goto H, Inagaki M, Oyama M,
814 Kitagawa D. 2014. Direct interaction of Plk4 with STIL ensures formation of a
815 single procentriole per parental centriole. *Nat Commun* 5:5267.
816 doi:10.1038/ncomms6267
- 817 Ohta M, Watanabe K, Ashikawa T, Nozaki Y, Yoshida S, Kimura A, Kitagawa D.
818 2018. Bimodal Binding of STIL to Plk4 Controls Proper Centriole Copy Number.
819 *Cell Reports* 23:3160-3169.e4. doi:10.1016/j.celrep.2018.05.030
- 820 Park J-E, Zhang L, Bang JK, Andresson T, DiMaio F, Lee KS. 2019. Phase
821 separation of Polo-like kinase 4 by autoactivation and clustering drives centriole
822 biogenesis. *Nat Commun* 10:4959. doi:10.1038/s41467-019-12619-2
- 823 Park S-Y, Park J-E, Kim T-S, Kim JH, Kwak M-J, Ku B, Tian L, Murugan RN, Ahn M,
824 Komiya S, Hojo H, Kim N-H, Kim BY, Bang JK, Erikson RL, Lee KW, Kim SJ, Oh
825 B-H, Yang W, Lee KS. 2014. Molecular Basis for Unidirectional Scaffold Switching
826 of Human Plk4 in Centriole Biogenesis. *Nat Struct Mol Biol* 21:696–703.
827 doi:10.1038/nsmb.2846
- 828 Pelletier L, O’Toole E, Schwager A, Hyman AA, Müller-Reichert T. 2006. Centriole
829 assembly in *Caenorhabditis elegans*. *Nature* 444:619–623.
830 doi:10.1038/nature05318
- 831 Raaijmakers JA, Heesbeen RGHP van, Meaders JL, Geers EF, Fernandez-Garcia
832 B, Medema RH, Tanenbaum ME. 2012. Nuclear envelope-associated dynein
833 drives prophase centrosome separation and enables Eg5-independent bipolar
834 spindle formation. *Embo J* 31:4179–4190. doi:10.1038/emboj.2012.272
- 835 Robinson JT, Wojcik EJ, Sanders MA, McGrail M, Hays TS. 1999. Cytoplasmic
836 dynein is required for the nuclear attachment and migration of centrosomes during
837 mitosis in *Drosophila*. *The Journal of cell biology* 146:597–608.

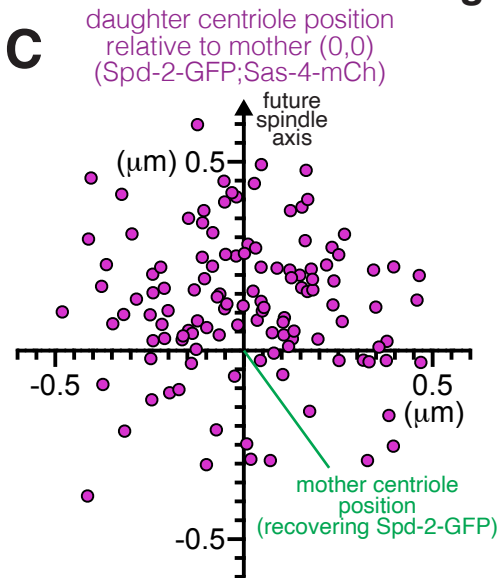
- 838 Rogers GC, Rusan NM, Roberts DM, Peifer M, Rogers SL. 2009. The SCFSlimb
839 ubiquitin ligase regulates Plk4/Sak levels to block centriole reduplication. *J Cell*
840 *Biology* 184:225–239. doi:10.1083/jcb.200808049
- 841 Salisbury JL, D'Assoro AB, Lingle WL. 2004. Centrosome Amplification and the
842 Origin of Chromosomal Instability in Breast Cancer. *J Mammary Gland Biol*
843 9:275–283. doi:10.1023/b:jomg.0000048774.27697.30
- 844 Sillibourne JE, Tack F, Vloemans N, Boeckx A, Thambirajah S, Bonnet P,
845 Ramaekers FCS, Bornens M, Grand-Perret T. 2010. Autophosphorylation of polo-
846 like kinase 4 and its role in centriole duplication. *Mol Biol Cell* 21:547–561.
847 doi:10.1091/mbc.e09-06-0505
- 848 Slevin LK, Romes EM, Dandulakis MG, Slep KC. 2014. The Mechanism of Dynein
849 Light Chain LC8-mediated Oligomerization of the Ana2 Centriole Duplication
850 Factor. *J Biol Chem* 289:20727–20739. doi:10.1074/jbc.m114.576041
- 851 Sonnen KF, Gabryjonczyk A-M, Anselm E, Stierhof Y-D, Nigg EA. 2013. Human
852 Cep192 and Cep152 cooperate in Plk4 recruitment and centriole duplication. *J*
853 *Cell Sci* 126:3223–3233. doi:10.1242/jcs.129502
- 854 Splinter D, Tanenbaum ME, Lindqvist A, Jaarsma D, Flotho A, Yu KL, Grigoriev I,
855 Engelsma D, Haasdijk ED, Keijzer N, Demmers J, Fornerod M, Melchior F,
856 Hoogenraad CC, Medema RH, Akhmanova A. 2010. Bicaudal D2, dynein, and
857 kinesin-1 associate with nuclear pore complexes and regulate centrosome and
858 nuclear positioning during mitotic entry. *Plos Biol* 8:e1000350.
859 doi:10.1371/journal.pbio.1000350
- 860 Stevens NR, Dobbelaere J, Brunk K, Franz A, Raff JW. 2010. Drosophila Ana2 is a
861 conserved centriole duplication factor. *J Cell Biology* 188:313–323.
862 doi:10.1083/jcb.200910016
- 863 Takao D, Yamamoto S, Kitagawa D. 2019. A theory of centriole duplication based on
864 self-organized spatial pattern formation. *J Cell Biol* 218:3537–3547.
865 doi:10.1083/jcb.201904156
- 866 Tang CC, Lin S, Hsu W, Lin Yi-Nan, Wu C, Lin Yu-Chih, Chang C, Wu K, Tang TK.
867 2011. The human microcephaly protein STIL interacts with CPAP and is required
868 for procentriole formation. *Embo J* 30:4790–4804. doi:10.1038/emboj.2011.378
- 869 Terra SL, English CN, Hergert P, McEwen BF, Sluder G, Khodjakov A. 2005. The de
870 novo centriole assembly pathway in HeLa cells cell cycle progression and
871 centriole assembly/maturation. *J Cell Biology* 168:713–722.
872 doi:10.1083/jcb.200411126
- 873 Wang C, Li S, Januschke J, Rossi F, Izumi Y, Garcia-Alvarez G, Gwee SSL, Soon
874 SB, Sidhu HK, Yu F, Matsuzaki F, Gonzalez C, Wang H. 2011. An ana2/ctp/mud

- 875 complex regulates spindle orientation in *Drosophila* neuroblasts. *Dev Cell* 21:520
876 533. doi:10.1016/j.devcel.2011.08.002
- 877 Woodruff JB, Wueseke O, Hyman AA. 2014. Pericentriolar material structure and
878 dynamics. *Philosophical Transactions Royal Soc B Biological Sci* 369:20130459.
879 doi:10.1098/rstb.2013.0459
- 880 Yamamoto S, Kitagawa D. 2021. Emerging insights into symmetry breaking in
881 centriole duplication: updated view on centriole duplication theory. *Curr Opin*
882 *Struc Biol* 66:8–14. doi:10.1016/j.sbi.2020.08.005
- 883 Yamamoto S, Kitagawa D. 2019. Self-organization of Plk4 regulates symmetry
884 breaking in centriole duplication. *Nat Commun* 10:1810. doi:10.1038/s41467-019-
885 09847-x
- 886

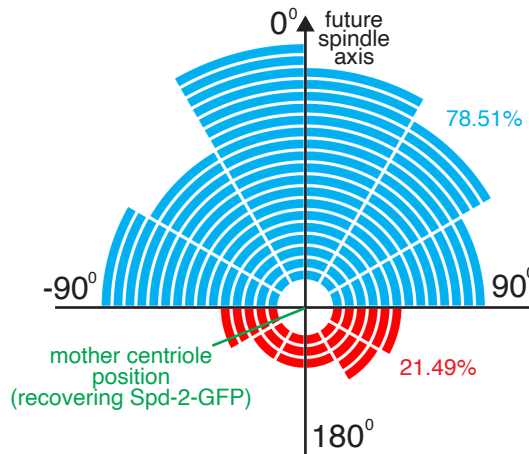
Figure 1



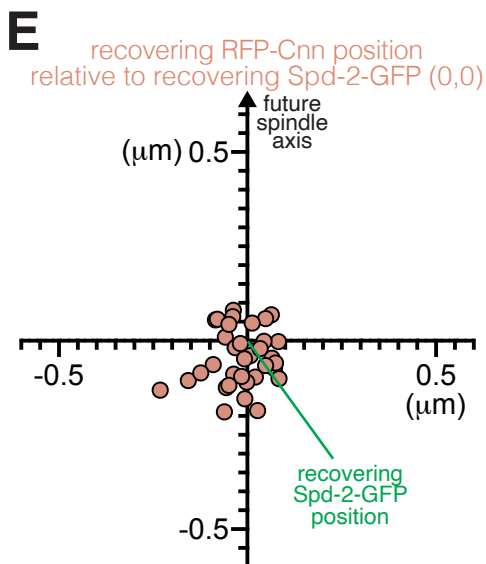
mother-daughter experiment



D rose plot for daughter centriole angle relative to future spindle axis (Spd-2-GFP; Sas-4-mCh)



mother-mother control



F rose plot of angles between recovering RFP-Cnn position and recovering Spd-2-GFP position

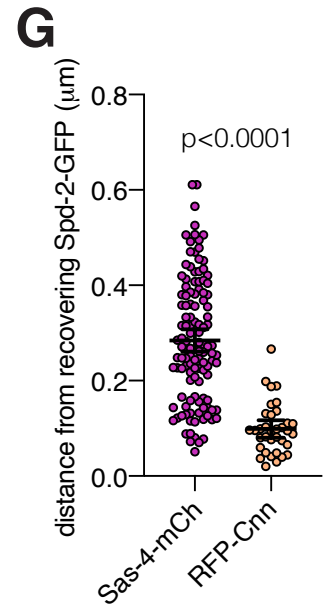
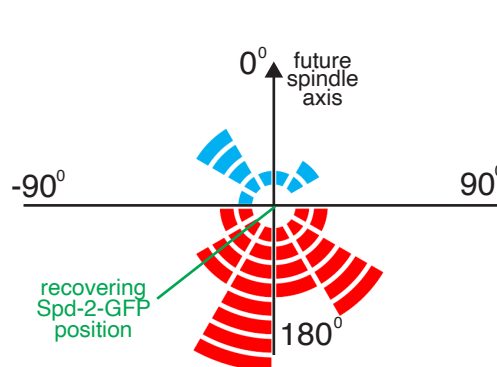
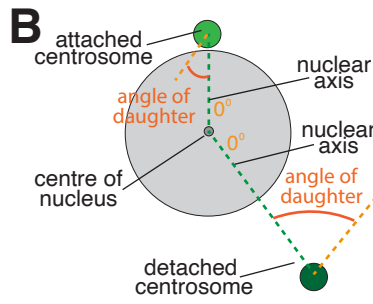
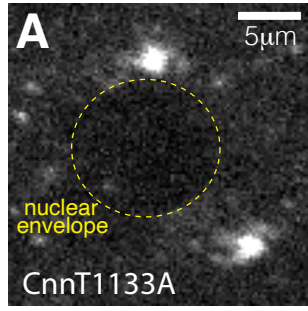
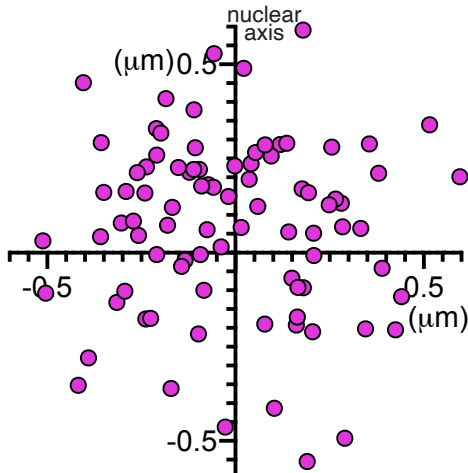


Figure 2

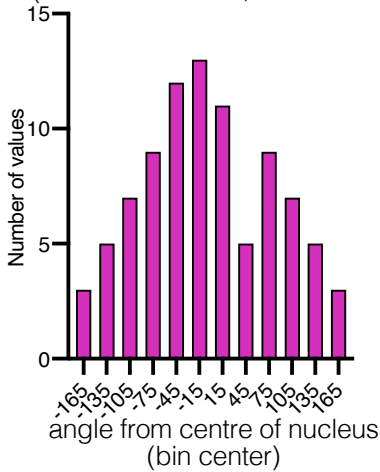


attached centrosomes

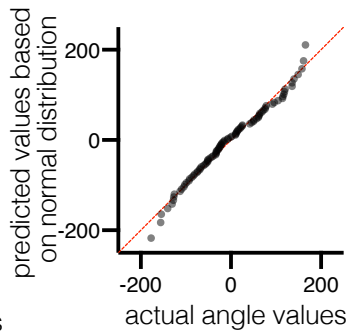
C daughter centriole position relative to mother centriole (0,0) and nuclear axis (GFP-CnnT1133A; Sas-4-mCh)



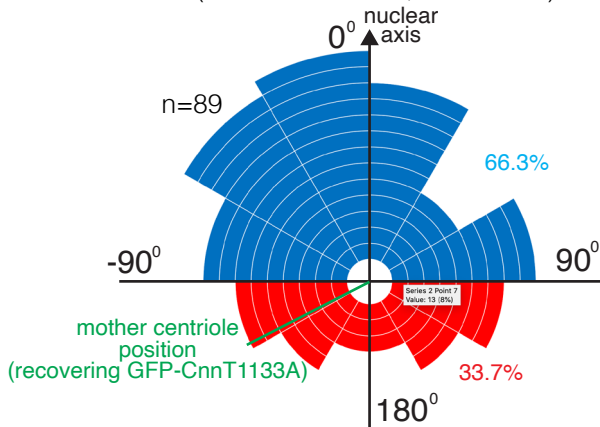
D Frequency distribution of daughter centriole angles relative to nuclear axis (GFP-CnnT1133A; Sas-4-mCh)



E normal QQ plot for angles (GFP-CnnT1133A; Sas-4-mCh)

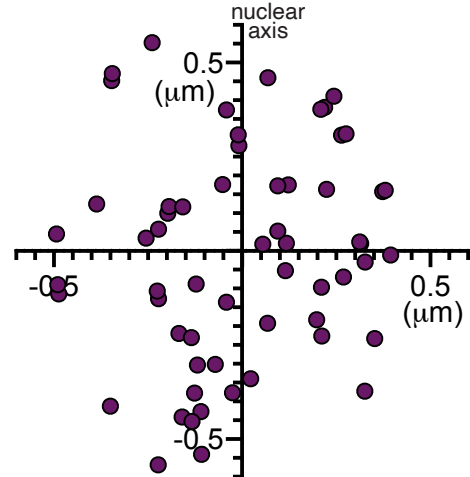


F rose plot for daughter centriole angle relative to nuclear axis (GFP-CnnT1133A; Sas-4-mCh)

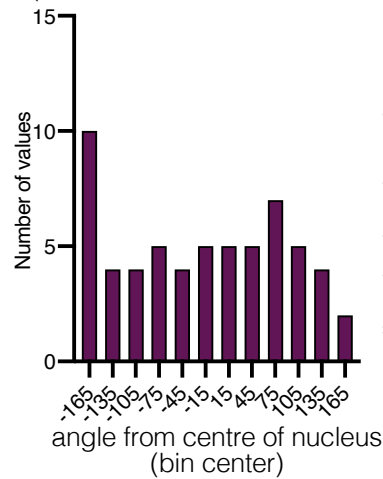


detached centrosomes

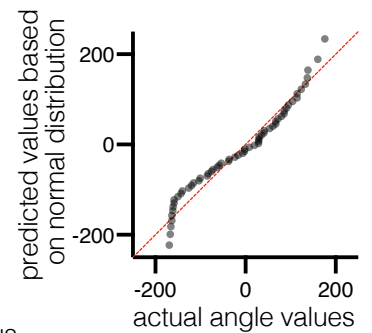
G daughter centriole position relative to mother centriole (0,0) and nuclear axis (GFP-CnnT1133A; Sas-4-mCh)



H Frequency distribution of daughter centriole angles relative to nuclear axis (GFP-CnnT1133A; Sas-4-mCh)



I normal QQ plot for angles (GFP-CnnT1133A; Sas-4-mCh)



J rose plot for daughter centriole angle relative to nuclear axis (GFP-CnnT1133A; Sas-4-mCh)

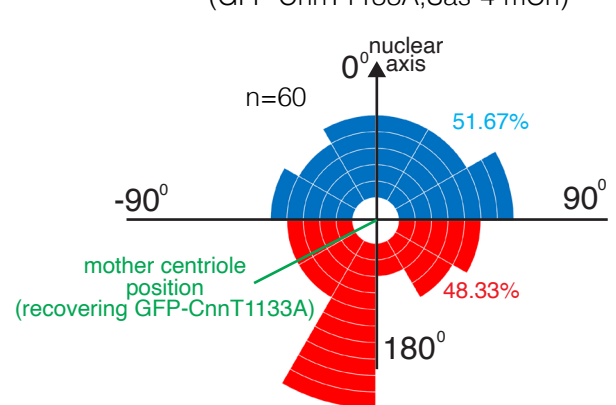


Figure 3

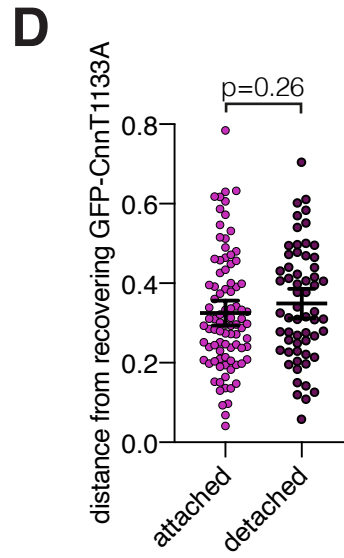
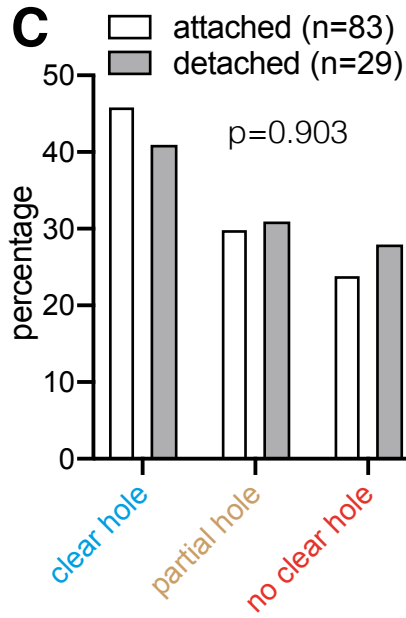
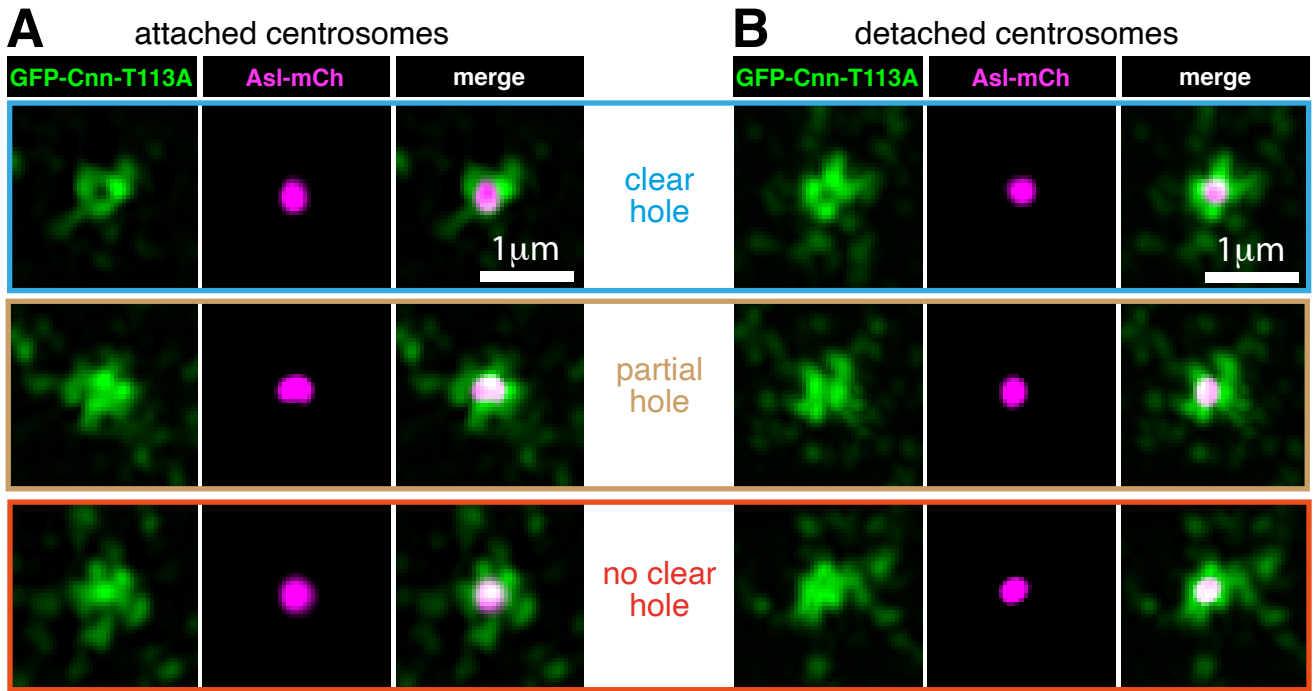
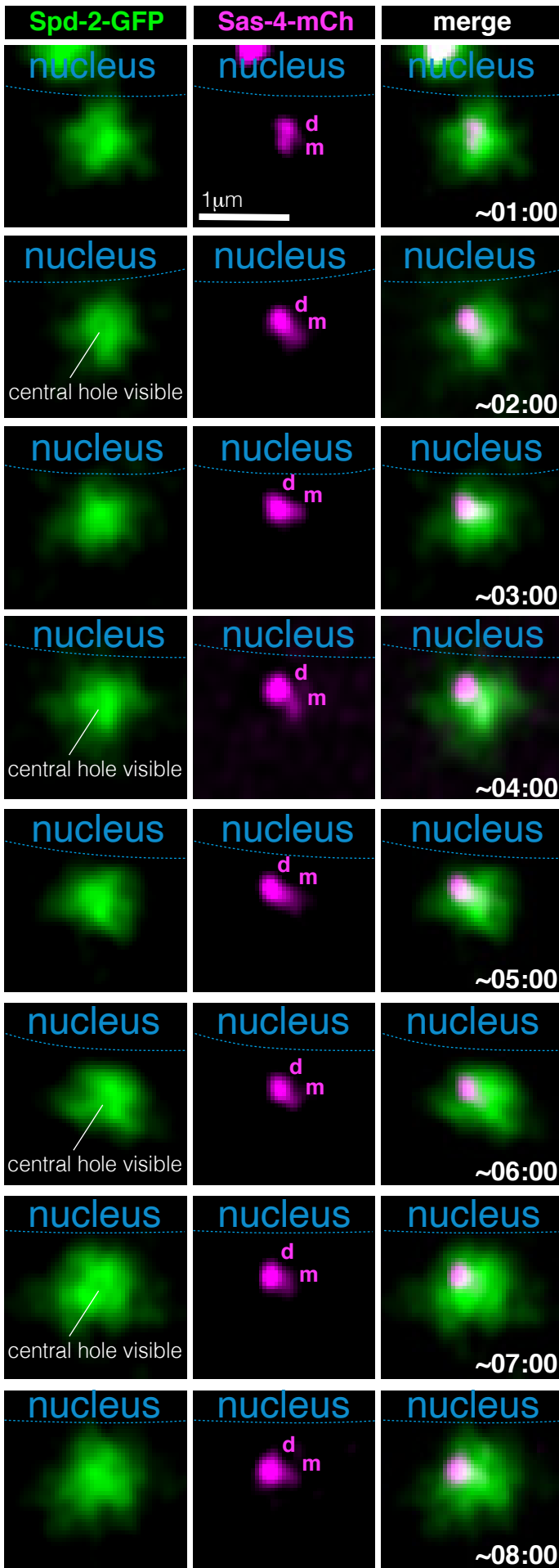
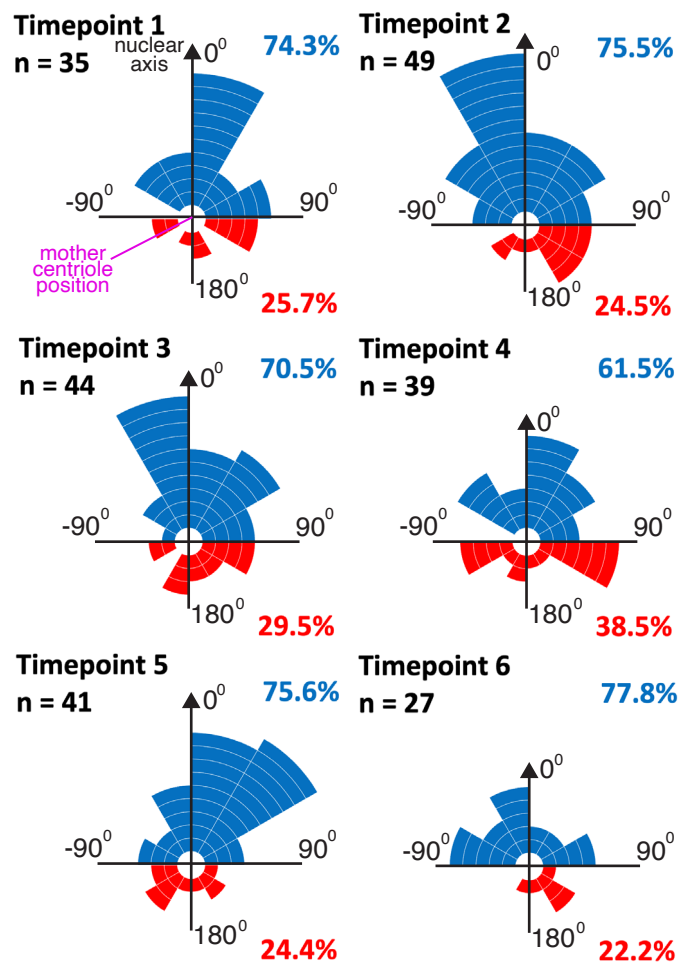


Figure 4

A



B



C

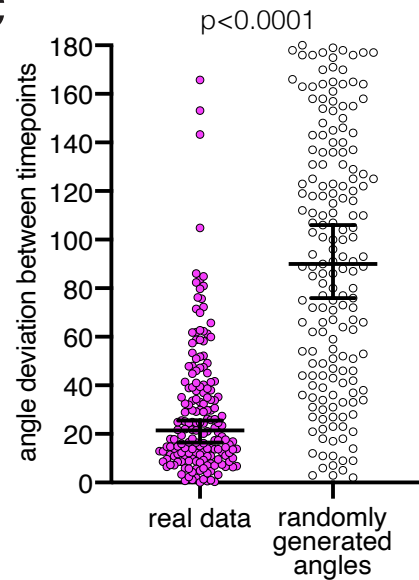
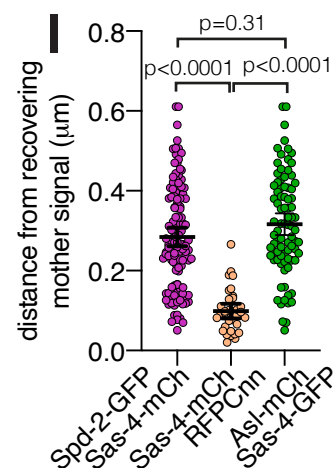
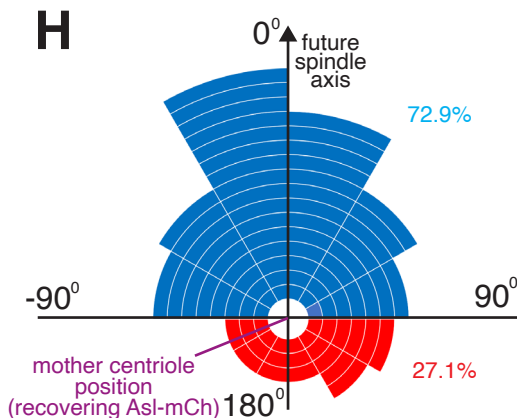
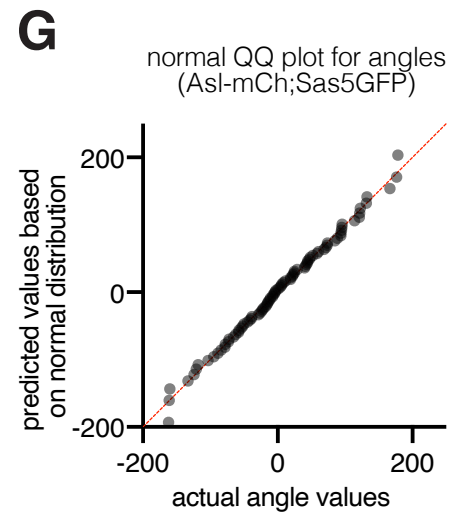
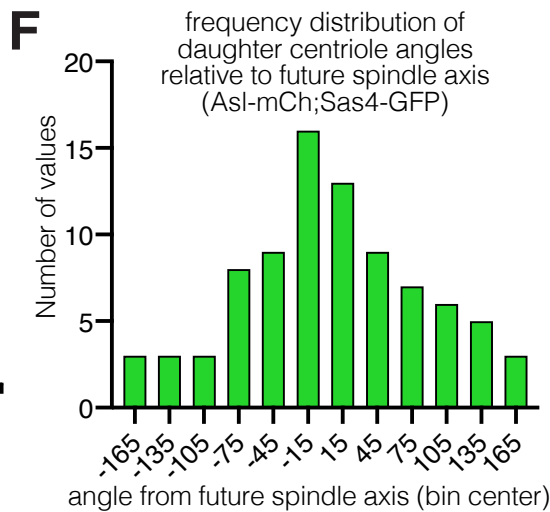
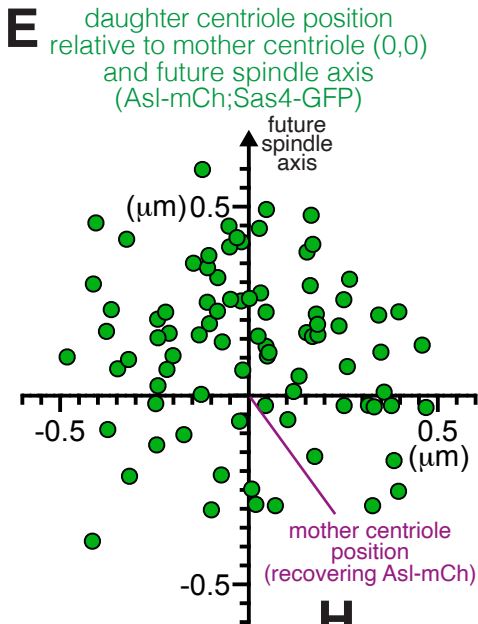
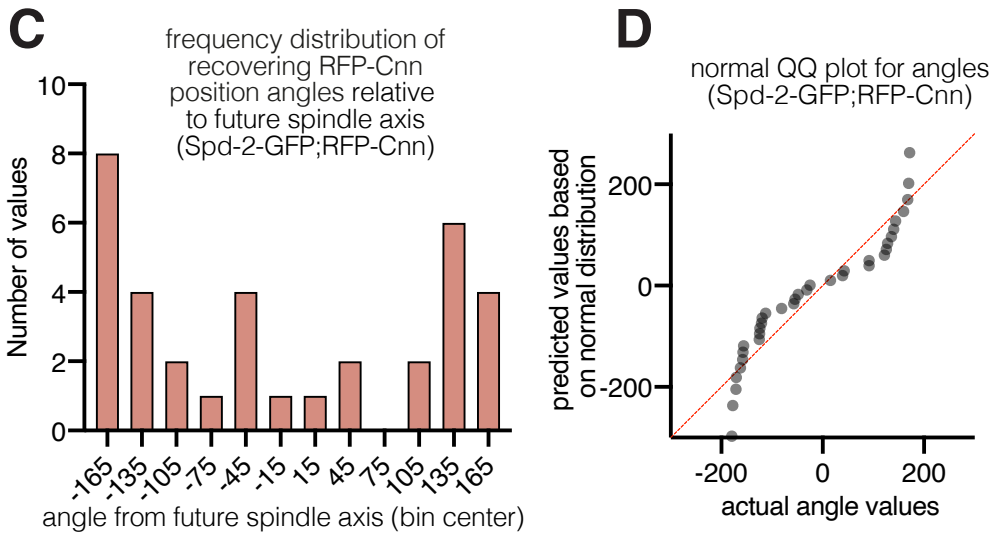
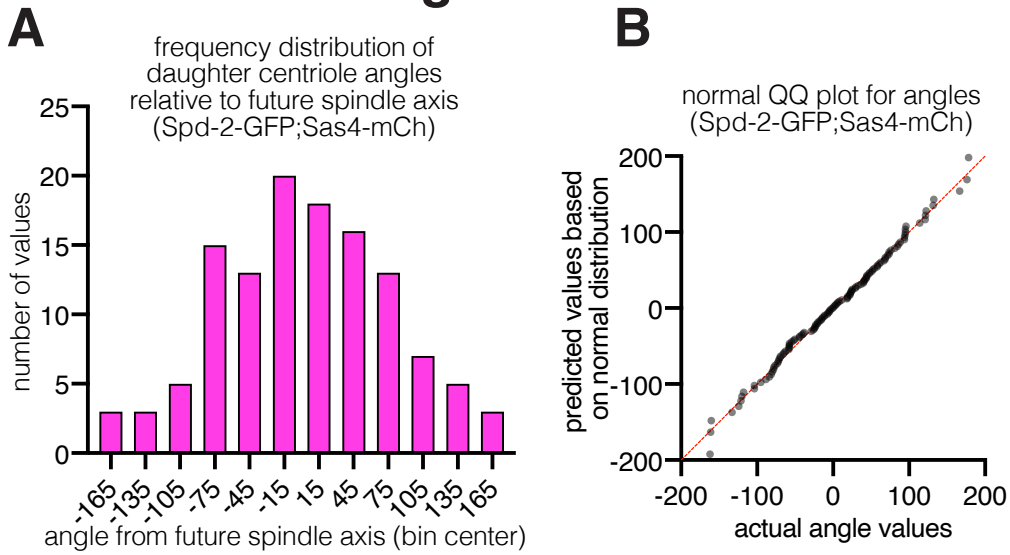


Figure S1



Online Supplementary Material

Figure S1

Further analysis of dual-colour FRAP data supports the finding that the site of daughter centriole assembly is non-random. (A) Frequency distribution of the angles at which daughter centrioles (marked by Sas-4-mCherry) form in relation to the future spindle axis (0°). (B) Normal QQ plot showing that the angles in (A) conform well to a normal distribution. (C) Frequency distribution of the angles at which the recovering RFP-Cnn fluorescence is positioned in relation to the future spindle axis (0°). (D) Normal QQ plot showing that the angles in (B) do not conform well to a normal distribution. (E) Graph displays the estimated positions of daughter centrioles (green circles) relative to the estimated position of their respective mother centrioles (position 0,0 on the graph) and the future spindle axis (positive y-axis) obtained from Asl-mCherry (mother) Sas-4-GFP (daughter) data. (F) Frequency distribution of the angles at which daughter centrioles (marked by Sas-4-GFP) form in relation to the future spindle axis (0°). (G) Normal QQ plot showing that the angles in (F) conform well to a normal distribution. (H) Rose plot representing the angle at which daughter centrioles (marked by Sas-4-GFP) form in relation to the future spindle axis (0°). Each segment corresponds to a single duplication event. Blue and red segments indicate daughter centriole assembly occurring less than or more than 90° from the future spindle axis, respectively. (I) Graph showing the distance between the estimated positions of mother and daughter centrioles (left and right datasets) or two different estimations of the mother centriole (central dataset) in the different imaging conditions used, as indicated. Note that data for the datasets on the left and in the centre have been re-plotted from Figure 1G to allow comparison to the dataset on the right. Datasets were compared to each other using a one-way ANOVA Kruskal-Wallis test.

Figure S1

